

# Physical factors determining the particle spatial orientation in ice clouds

B.V. Kaul<sup>1</sup> and I.V. Samokhvalov<sup>2</sup>

<sup>1</sup>*Institute of Atmospheric Optics,  
Siberian Branch of the Russian Academy of Sciences, Tomsk*  
<sup>2</sup>*Tomsk State University*

Received June 20, 2007

The aerodynamic and electrostatic effects on the cloud ice particles have been considered. The plate- and column-shaped cloud particles are modeled as oblate spheroids and prolate rotational ellipsoids. We obtained the formulas for functions of the size distribution over the angles of polar and azimuthal orientation in the polydisperse ensembles of the plate and columnar particles in the case of the combined effect of aerodynamic and electrostatic effect on them under the conditions of destructive influence on the process of the orientation from thermal motion of air molecules and air turbulence.

## Introduction

Transmission and scattering of solar radiation by ice clouds strongly depend on the spatial particle orientation. Because the ice clouds markedly influence the radiation balance of the surface – atmosphere system, a correct accounting for the particle orientation in the solution of problems of solar radiative transfer in the atmosphere seems to be urgent. Nonetheless, to the recent time the solution of this problem cannot be considered substantially advanced. Even relatively recent calculations used the models of three- or two-dimension random particle orientation or the Gaussian distribution over orientation angles of large-diameter particles in the near-horizontal position.<sup>1–4</sup> However, in the last case it is unclear, which dispersion should be considered as a distribution parameter. For quite clear reasons, the experimental information on the cloud particle orientation, obtained *in situ*, is absent. There are only individual laboratory studies of fall speed and orientation of the ice crystals.<sup>5,6</sup>

In Refs. 7 and 8 heuristic models of the process of particle orientation during their fall were proposed. The question on destructive influence of turbulent air motions on the particle orientation turned out to be most debatable. Whereas in Ref. 7 any influence of turbulence on the orientation is virtually denied, the analysis in Ref. 8 has shown that the turbulence markedly influences the large-diameter particle distribution around the horizontal position. The experimental data usable to judge the validity of one or another model have long been absent.

Our results of lidar measurements of the backscattering matrices<sup>9</sup> have allowed us to estimate the degree of particle orientation by large diameters in the horizontal position. It was found that this orientation is generally less pronounced than model estimates show.<sup>8</sup>

Moreover, the measurements have shown the presence of predominately poorly defined azimuthal particle orientation, that is ignored by existing models. We showed that one of the reasons for such an orientation may be wind velocity pulsations.

The electrostatic fields in the clouds may exert orienting effect as well. The description of this type of orientation is closely related to the description of electro-optic effect in aerosol media. This phenomenon is widely studied in the literature. Some relevant references are presented in Ref. 13, however, the estimates of the influence of electro-optic fields on orientation of ice cloud particles are absent. As it will be shown below, the vertical gradients of electric potential prevent the horizontal orientation of particles with large diameters; and in case of quite strong fields may change the orientation type.

In the cycle of papers,<sup>10–12</sup> we considered separately the effects of aerodynamic and electrostatic orientation. It seems expedient here, avoiding the redundant mathematical detailing accessible in the cited references, to consider these effects in combination.

## Aerodynamic orientation

It is known from hydrodynamics that the body, located in the incoming flow of liquid or air, is influenced by the moment of forces, tending to rotate it by its largest size across the flow direction. This is an experimental fact. Its theoretical explanation can be found in the hydrodynamics literature.<sup>14,15</sup> The character of the motion with the body largest diameter oriented perpendicularly to the velocity vector of the incoming flow remains stable until the following condition is satisfied for the Reynolds numbers

$$Re = uh/\nu \gtrsim 50,$$

where  $u$  is the relative velocity of the body in the flow;  $\nu$  is the kinematic viscosity of air; and  $h$  is the

characteristic size, approximately equal to the largest diameter of the body. When  $Re \approx 50$ , there takes place the regime of shedding of eddies and the stable motion of particles with large diameters oriented across the direction of motion, is distorted. Simultaneously, oscillations about the position of the stable motion or chaotic rotations and “tumbling” of the body take place. All this is well described in Ref.16, where the results of numerical solution of Navier–Stokes equation are presented for the case of cylinder fall for different numbers  $Re$ . The same reference presented the photos with visualization of eddy motions during fall of cylindrical body in liquid.

### Particle orientation during fall

The orientation of ice cloud particles by large diameters in the horizontal position, when falling, is the basic and constantly acting factor. The regime of motion depends on the number  $Re$  magnitude. The fall speed depends on the particle mass and shape. For spherical micron-sized particles, the fall speed can be determined from the Stokes formula

$$mg = 6\pi\eta r, \quad (1)$$

where  $m$  is the particle mass;  $g$  is the acceleration of gravity;  $\eta$  is the dynamical viscosity of air ( $\text{kg} \cdot \text{m}^{-1} \cdot \text{s}^{-1}$ ); and  $r$  is the particle radius.

This formula is valid for regime of the viscous motion. In the regime of motion with formation of eddies, it gives overestimated results. In this case, it is expedient to use the empirical formula<sup>17</sup>:

$$u = Ah^\beta. \quad (2)$$

Values of the empirical constants  $A$  and  $\beta$  for plate and columnar particles are given in Ref. 17 as well. In the range of sizes  $h$  from 5 to 20  $\mu\text{m}$ , formulas (1) and (2) give approximately identical results (from 0.5 to 4  $\text{cm/s}$ ). The size spectrum of the ice particles extends from a few microns to a few millimeters.<sup>18</sup> It is important that throughout this interval the regime of motion with the eddy shedding is absent.<sup>10</sup> In this case, we can use the well-known<sup>15</sup> formula for the moment of forces, acting on the oblate spheroid or prolate ellipsoid, whose small semiaxes are deflected by the angle  $\theta$  from the direction of motion:

$$M_a(\theta) = -\frac{\partial U_a}{\partial \theta} = [-\lambda u^2 \rho V \sin 2\theta]/2, \quad (3)$$

where  $M_a$  is the moment of forces which, by the mechanics rules, is equal to the oppositely signed derivative of the potential energy; the subscript “a” means “aerodynamic”;  $\rho$  is the air density;  $V$  is the particle volume;  $\lambda$  is the form factor which depends on the type and eccentricity of the particle. Here, following other authors, we have to replace the plate crystals and columns, respectively, by oblate spheroids and prolate ellipsoids, because the form factors are theoretically determined only for them.<sup>15</sup> Formulas for their calculation are given in Ref. 10.

### Orientation due to wind velocity pulsations

Experimental studies of the backscattering matrices of ice clouds<sup>9</sup> have shown that the particles of these clouds, in addition to their orientation by large diameters in the horizontal plane, may also be oriented in azimuth. That is, the large diameters may be predominately concentrated around some direction in the horizontal plane. Earlier, there were only indirect evidences of the possibility of such an orientation. They relied upon the observation of such a rare phenomenon as inclined sun pillars. Possible mechanisms of the azimuthal orientation were never considered before. We hypothesized that one of the reasons for such an orientation may be wind velocity pulsations. As we have shown earlier,<sup>11</sup> this is possible if the Lagrange integrated timescales of the longitudinal and transverse pulsations substantially differ. That is, the orientation may be determined by the pulsations belonging to the region of anisotropic turbulence, preserving the wind orientation. In this case, the pulsations of the particle velocity, due to inertia, are shifted in phase and differ in the amplitude relative to the pulsations of airflow velocity. The orienting moment follows from Eq. (3), if the squared fall velocity is replaced by the mean squared difference of velocities of pulsations of air and particle  $\delta u$ :

$$M(\varphi) = [-\lambda \langle (\delta u)^2 \rangle \gamma \rho V \sin 2\varphi]/2, \quad (4)$$

where  $\varphi$  is the deviation angle of the small axis of ellipsoid of rotation from the mean wind direction; and  $\gamma$  is the anisotropy factor of turbulent pulsations (it was equal to 0.5 in Ref.11). The mean square of the difference of pulsation rates is determined by the formula

$$\langle (\delta u)^2 \rangle = \frac{1}{2T} \int_0^T \int_{\omega_0}^{\omega_T} \varepsilon \omega^{-2} \left[ \sin \omega t - \sin(\omega t - \phi) \right] / \sqrt{1 - \omega^2 \tau_0^2} d\omega, \quad (5)$$

where  $\varepsilon$  is the energy dissipation rate,  $\text{m}^2/\text{s}^3$ ;  $\phi = \arctan \omega \tau_0$  is the phase shift; and  $\omega_0 = 1/\tau_0$ .

The integration is conducted over the interval of the effective frequencies. The lower bound of the interval is determined by the characteristic time  $\tau_0$  of the largest particles. It characterizes the inertial property of particles. For oblate spheroids and prolate ellipsoids,

$$\tau_0 = \rho_p h^2 \sqrt{1 - e^2} / 15\eta, \quad \tau_0 = \rho_p h^2 (1 - e^2) / 12\eta, \quad (6)$$

where  $\rho_p$  is the density of the particle substance; and  $e$  is the eccentricity.

If the frequencies of the air pulsations  $\omega < \omega_0$ , then the particle can be considered fully carried away so  $\delta u = 0$ . The interval of  $\tau_0$  variations for ice particles is quite wide and ranges from  $10^{-4}$  s for particles with sizes about 10  $\mu\text{m}$  and 1–2 s for particles as large as 1 mm.

The upper integration limit is defined as the frequency of the Taylor microscale<sup>19</sup>:

$$\omega_T = \sqrt{\varepsilon/15\nu}. \quad (7)$$

Depending on the turbulence intensity, it varies approximately from 2 to 15 rad/s. This corresponds to timescales 0.5–0.07 s. Particles, whose characteristic time  $\tau_0$  is less than 0.05 s, which corresponds approximately to sizes of 150  $\mu\text{m}$ , can be considered totally carried away even for strongly developed turbulence. This means that the orientation, determined by wind pulsations, is effective for larger particles. In fact, as is shown in Ref. 11, a sufficiently effective orientation can take place for columns with the length larger than 500  $\mu\text{m}$ . At the same time, the column axes tend to orient perpendicularly to the wind direction. The degree of orientation is generally not large.<sup>11</sup>

The plate's base surfaces should be oriented perpendicularly to the wind direction. Then, in addition to the action of the moment of forces (3), they should be influenced by the moment

$$M(\theta) = [-\lambda \langle (\delta u)^2 \rangle \gamma \rho V \sin 2(\pi/2 + \theta)]/2. \quad (8)$$

When moments (3) and (8) act simultaneously, the plates must come to inclined position with respect to the horizontal plane. Moreover, the inclination has to be predominately in one direction, namely in the wind direction. This effect could explain the appearance of inclined sun pillars.<sup>20</sup> However, the square of the fall velocity is almost three orders of magnitude larger than  $\langle (\delta u)^2 \rangle$  even in the case of the strongly developed turbulence ( $\varepsilon = 10^{-1}$ ). Therefore, the inclination angle, at which the moments (3) and (8) are balanced, does not exceed a few milliradians. Hence, the action of wind velocity pulsations on orientation of plate-shaped particles should be considered negligible.

### Azimuthal orientation as a consequence of particle fall in the presence of the wind velocity vertical gradient

If there is a vertical gradient of wind velocity  $\partial v_x / \partial z$ , then during the particle fall its horizontal velocity component, depending on the sign of the gradient, is larger or smaller than the airflow velocity. The velocity difference is expressed by the formula

$$\delta u = \frac{\partial v_x}{\partial z} u_z \tau_0, \quad (9)$$

where  $u_z$  is the fall velocity. The quantity  $\delta u$ , defined in such a way, should be substituted in formula (8) with simultaneous excluding the anisotropy factor  $\gamma$  from it. The estimates from Ref. 11 show that for all conceivable gradients of the vertical velocity this orientation mechanism is much less efficient than the process of orientation with the help of wind pulsations. Therefore, further it will not be taken into consideration.

## Orientation of ice particles by electrostatic fields of the atmosphere

In a particle made of dielectric material and placed into the static electric field with intensity  $\mathbf{E}$ , the dipole moment  $\mathbf{p}$  is induced. If the dielectric susceptibility of the dielectric is scalar, and the particle has a near-spherical shape, then the direction of the dipole moment coincides with the direction of the field, and the potential energy of the “dipole – field” system

$$U = -\mathbf{p}\mathbf{E} \quad (10)$$

is equal to the decrease of the electrostatic field energy. In this case, the external moments of forces do not act on the particle. However, if its dielectric susceptibility is a tensor quantity, or the polarizability is different for different directions because of the particle nonsphericity, even if it is an isotropic dielectric, then the potential energy will depend on the particle position. In the general case, it will be under action of the moment of forces, tending to rotate the particle to the position, at which its potential energy is minimal.

The relative dielectric constant  $\varepsilon'$  of the clean ice in the static field is very large and equals 73 [Ref. 21]. Correspondingly, the dielectric susceptibility  $\chi = \varepsilon' - 1 = 72$ . The small anisotropy of the dielectric susceptibility, manifesting itself as birefringence at optical frequencies, in the static field does not play a significant role. The anisotropy of polarizability of ice particles is determined by the anisometry of their sizes. As before, we model the plates and the columns, respectively, as strongly oblate spheroids and prolate ellipsoids of rotation. For bodies of this shape, the components of the dipole moment can be written as follows:

$$\begin{aligned} p_{\perp} &= \varepsilon_0 \alpha_{\perp} V = \varepsilon_0 \chi / (1 + \kappa_{\perp} \chi) V E_{\perp}, \\ p_{\parallel} &= \varepsilon_0 \alpha_{\parallel} V = \varepsilon_0 \chi / (1 + \kappa_{\parallel} \chi) V E_{\parallel}, \end{aligned} \quad (11)$$

where  $\varepsilon_0$  is the electric constant; symbols  $\perp$ ,  $\parallel$  mean “perpendicular” and “parallel” to the rotation axis of spheroid or ellipsoid; and  $\kappa_{\perp}$ ,  $\kappa_{\parallel}$  are form factors. Their form and formula for calculations are presented in Ref. 12. Here, we only note that for prolate ellipsoids  $\alpha_{\parallel} > \alpha_{\perp}$ , while for spheroids  $\alpha_{\parallel} < \alpha_{\perp}$ .

The potential energy of the bodies of the above-mentioned shapes is determined by the formula<sup>12,13</sup>:

$$U_e(\theta) = -\frac{1}{2} \varepsilon_0 V (\alpha_{\perp} \sin^2 \theta + \alpha_{\parallel} \cos^2 \theta) \mathbf{E}^2, \quad (12)$$

where  $\theta$  is the angle between the direction of the vector  $\mathbf{E}$  and the axis of rotation of ellipsoid (spheroid).

In the electric field the particle takes such a position, in which the potential energy is minimal, and the acting moment of the forces turns to be zero. The second derivative, according under the condition of minimum, must be positive:

$$\frac{\partial U_e}{\partial \theta} = -\frac{1}{2}\varepsilon_0 V E^2 (\alpha_{\perp} - \alpha_{\parallel}) \sin 2\theta = -M_e(\theta) = 0, \quad (13)$$

$$\frac{\partial^2 U_e}{\partial \theta^2} = -\varepsilon_0 V E^2 (\alpha_{\perp} - \alpha_{\parallel}) \cos 2\theta > 0.$$

In the case of prolate ellipsoids,  $\alpha_{\parallel} > \alpha_{\perp}$  and conditions (13) are fulfilled at  $\theta = 0$ . The rotation axis of spheroids becomes oriented perpendicular to the vector  $\mathbf{E}$  ( $\theta = \pi/2$ ). In any case, the particle is positioned by its longer diameter along the field vector.

### Destructive influence of thermal motion and turbulence on the particle orientation

Brownian rotation and the influence of collective motion of the molecules in turbulent cells of energy dissipation scale, whose sizes are comparable with particle sizes, must shift particles from position corresponding to the minimum of potential energy. The larger-scale collective motions can change the momentum of the particle, but not its angular momentum. The energy  $kT$  is transferred to two rotational degrees of freedom. The rotation around main axis of symmetry of spheroid or ellipsoid of rotation is not of importance in this problem.

According to Kolmogorov model of turbulence, scales of sizes and velocity in the interval of energy dissipation are, respectively

$$l_0 = \left(\frac{v^3}{\varepsilon}\right)^{1/4}, \quad u_t = (\varepsilon v)^{1/4}. \quad (14)$$

As  $\varepsilon$  changes from  $10^{-4}$  to  $10^{-1}$ , the value of  $l_0$  changes approximately from 3 to 0.5 mm. The energy dissipation process is most intensive in the region  $0.1 < kl < 1$ , where  $k$  is the wavenumber and  $l$  is the cell size. This corresponds to sizes from  $6l_0$  to  $60l_0$  [Ref. 18].

Cell with diameter  $l_0$ , on average, possesses the energy

$$w = \frac{1}{6}\pi l_0^3 \rho \langle u_t^2 \rangle = w(\varepsilon) = \frac{1}{6}\pi \rho v^{11/4} \varepsilon^{-1/4}. \quad (15)$$

It is assumed that the efficiency of the energy transfer from the cell to the particle is proportional to the ratio of the particle volume to the volume of the cell with size  $l_0$ :

$$p(\varepsilon, h) \approx h^3 (v^3 / \varepsilon)^{-3/4}. \quad (16)$$

This assumption in essence contains one of the disagreements with the Klett model,<sup>8</sup> according to which the efficiency of the particle interaction with the cell is  $p \approx (h/l_0)^2$ , when  $h < l_0$ , и  $p \approx (h/l_0)^{3/2}$ , when  $h > l_0$ . We assume  $p \approx (h/l_0)^3$ . If the particle size is substantially less than  $l_0$ , which is true, e.g., for cirrus cloud particles even for quite developed

( $\varepsilon \leq 2 \cdot 10^{-3}$ ) turbulence, then, after it falls within the cell, it interacts only with a small volume of air in the cell, whereas the dependence  $p \approx (h/l_0)^2$  implies comparability of the surface areas. However, a small particle cannot influence essentially the air motion at the cell periphery. At  $\varepsilon \geq 2 \cdot 10^{-3}$ , the ice cloud particles become comparable with or even larger than  $l_0$ . These particles may interact with larger cells of the energy dissipation, having a larger energy. The multiplier  $(h/l_0)^3$  becomes equal to or larger than unity and takes into account this factor. We consider the presented arguments as convincing as those presented in Ref. 8. There are no reasons to expect exact estimates, relying on analysis of dimensions. It would be more correct to consider the parameter  $p(\varepsilon, h)$  as the fitting parameter, which could be refined experimentally. As it was already noted above, we refused from the Klett model<sup>8</sup> because it overestimates the degrees of orientation from the viewpoint of experiments.<sup>5,9</sup> The calculations of the particle orientation during fall, based on our model,<sup>10</sup> are compared with Klett results<sup>8</sup> in Fig. 1.

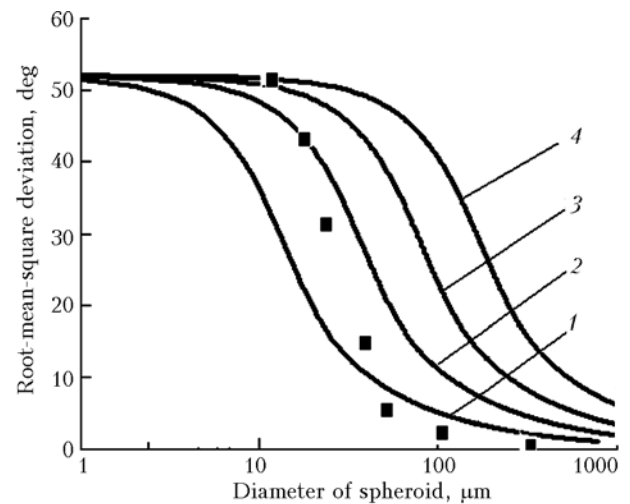


**Fig. 1.** Root-mean-square deviation of rotation axes of oblate (2.5 : 1) spheroids from vertical in distribution over orientations; the deviation arises due to action of aerodynamic moment of forces during fall and disorienting action of thermal motion of the molecules and turbulence at energy dissipation rates:  $\varepsilon = 0$  (curve 1),  $10^{-4}$  (curve 2),  $10^{-3}$  (curve 3), and  $10^{-2} - 10^{-1} \text{ m}^2/\text{s}^3$  (curve 4). Shown by squares are model results<sup>8</sup> for  $\varepsilon = 10^{-1}$ .

If in formula (16)  $h^3$  is expressed via particle volume:

$$h^3 = V_s / 6\pi \sqrt{1 - e^2} \quad \text{for spheroid}$$

and

$$h^3 = V_e / 6\pi(1 - e^2) \quad \text{for oblong ellipsoid,}$$

then from Eqs. (15) and (16) the kinetic energy, transferred to the particle from the turbulent motion, is written as

$$W(\varepsilon, V) = p\omega = \kappa_{s,e}^{-1} \rho V \sqrt{\varepsilon}, \quad (17)$$

where

$$\kappa_s = 6\pi\sqrt{1-e^2}, \quad \kappa_e = 6\pi(1-e^2).$$

Comparison of kinetic energies, received by the particle from thermal motion of the molecules and turbulent motion shows that the Brownian rotation prevails for micron-sized particles. The energy of turbulent motion becomes equal to it for particle sizes 8–10 μm. For larger particles, the energy transfer from turbulent cells prevails.

### Particle distribution over orientation angles during joint action of the aerodynamic moment of forces, arising during fall, and the moment caused by the electric potential gradient

#### Orientation in the presence of vertical gradient of electric field

The distribution can be found from the condition of balance between the increment of the potential energy of particles and the kinetic energy transported to them by turbulent pulsations and thermal motion

$$n(\theta)[\partial U_a / \partial \theta + \partial U_e / \partial \theta]d\theta + [W(\varepsilon, V) + kT]dn = 0. \quad (18)$$

Values of the potential energy derivatives are presented above (see Eqs. (3) and (13)).

Solution of this equation has the form

$$n(\theta, h) = C \exp[\xi(\varepsilon, h) \cos 2\theta], \quad (19)$$

where

$$\xi_s(\varepsilon, h) = \kappa_s \rho h^3 [\lambda_s(e) u_s^2(h) - \varepsilon_0 (\alpha_{\perp}^s - \alpha_{\parallel}^s) E^2] / 2(\rho h^3 \sqrt{\varepsilon} + kT) \quad (20)$$

for spheroids and

$$\xi_e(\varepsilon, h) = \kappa_e \rho h^3 [-\lambda_e(e) u_e^2(h) - \varepsilon_0 (\alpha_{\perp}^e - \alpha_{\parallel}^e) E^2] / 2(\rho h^3 \sqrt{\varepsilon} + kT)$$

for ellipsoids.

The multiplier  $C$  in Eq. (19) is determined from the normalization condition

$$\begin{aligned} d \int_{-\pi/2}^{\pi/2} n(\theta, h') d\theta &= N f(h') dh; \\ C &= N f(h') dh / \int_{-\pi/2}^{\pi/2} \exp[\xi(\varepsilon, h') \cos 2\theta] d\theta = \\ &= N f(h') dh / \pi I_0(\xi), \end{aligned}$$

where  $N$  is the total particle concentration;  $N f(h') dh$  is the number of particles with maximum diameter  $h'$  and diverse orientations falling within the size interval  $dh$ ;  $f(h)$  is the size distribution function

$\int_0^{\infty} f(h) dh = 1$ ;  $I_0(\xi)$  is  $0$ th-order Bessel function of the first kind.

The number of particles of arbitrary size, lying in the angle interval  $d\theta$  is given by the formula

$$n(\theta) d\theta = N d\theta \int_0^{\infty} \frac{\exp[\xi(\varepsilon, h) \cos 2\theta]}{\pi I_0[\xi(\varepsilon, h)]} f(h) dh. \quad (21)$$

Correspondingly, the quantity  $\Theta(\theta) = n(\theta) d\theta / N d\theta$  is the probability density of particle distribution over the angle  $\theta$ .

In the case of combined action of the aerodynamic moment of force and the moment, caused by the vertical gradient of electric potential, the distribution  $\Theta_{s,e}(\theta)$  is determined through substituting expressions for  $\xi$  from Eq. (20) to Eq. (21). As it follows from Eq. (20), the electrodynamic and electric moments of forces act in the opposite directions. For ellipsoids, this is because  $\alpha_{\perp} < \alpha_{\parallel}$ , while the minus in the first term in square brackets appears because  $\sin 2(\theta - \pi/2)$  should be used instead of  $\sin 2\theta$  in formula (3), because in the given problem, the angles are counted not up to the minimal diameters, but to the rotation axes. As an example, Figure 2 presents the pattern of the  $\Theta_s(\theta)$  distribution for spheroids with the ratio 2.5:1 of the maximal diameter to minimal one for four intensities of the electric field. The spheroids are distributed over sizes in accordance with the function presented in Fig. 3.

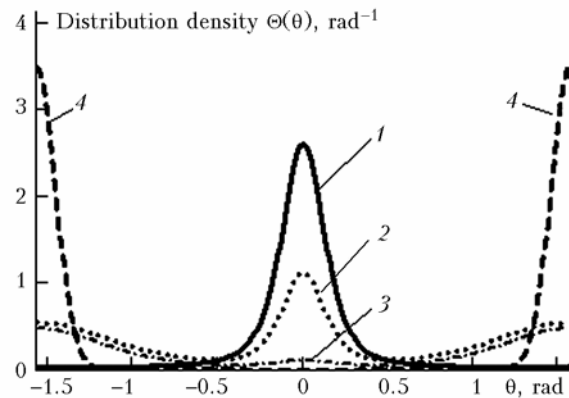


**Fig. 2.** Distribution of rotation axes of oblate (2.5 : 1) spheroids over polar angle  $\theta$  during joint action of aerodynamic and electrostatic moments of forces. The intensity of electric field  $E = 0$  (curve 1);  $4 \cdot 10^3$  (curve 2);  $10^4$  (curve 3); and  $1.5 \cdot 10^4$  V/m (curve 4) and directed vertically ( $\theta = 0$ ). The size distribution taken for the calculation is presented in Fig. 3.

At zero intensity of the electric field the distribution over orientation angles is determined only by the aerodynamic factor. The distribution mode  $\theta_m = 0$ , i.e., the rotation axes of spheroids are

predominately oriented vertically. As the intensity of the electric field  $E$  increases, the distribution becomes bimodal:  $\theta_m = 0, \theta_m = \pm \pi/2$ .

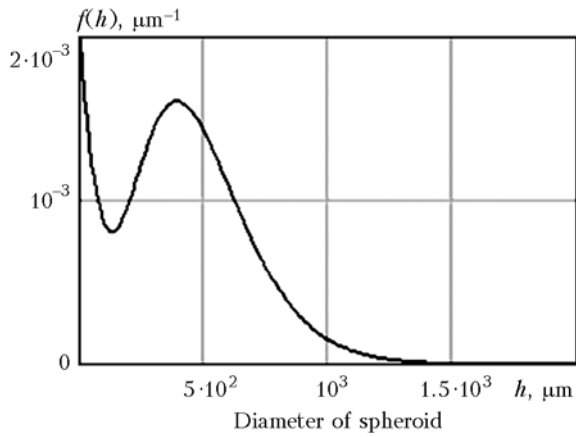


**Fig. 3.** The distribution of  $f(h)$  over largest diameters of spheroids, taken for the calculations presented in Fig. 2.

As follows from Eq. (20), the second term in square brackets does not depend on sizes, while the fall rate and, correspondingly, aerodynamic moment of forces is larger for bigger particles. Therefore, firstly small particles and then larger particles pass to the electric type of orientation  $\theta_m = \pm \pi/2$ . As  $E$  further grows, all particles become distributed according to  $\theta_m = \pm \pi/2$ , when rotation axes of spheroids are oriented horizontally. With increase of intensity of the field, the prolate ellipsoids of rotation change distribution from  $\theta_m = \pm \pi/2$  to  $\theta_m = 0$ . Their axes take predominately vertical positions.

**Orientation in the presence of horizontal gradient of electric field**

The presence of the vertical gradient is the most probable state of the electric field of the Earth. However, in the clouds the horizontal gradients are possible because of the cellular structure of distribution of charges.<sup>22</sup> Let us demonstrate the combined action of horizontal gradient of electric potential and aerodynamic moment of forces, acting during particle fall.

Define the coordinate system in such a way that the  $x$  axis has the direction of the intensity vector, while  $z$  axis is vertical. The positions of rotation axis of spheroid and ellipsoid of rotation are defined by  $\theta$  counted off the  $z$  axis and by  $\varphi$  measured from the  $x$  axis to projection of rotation angle onto the horizontal plane.

The potential energy in this case is defined by the formula<sup>13</sup>:

$$U_e(\theta) = -\frac{1}{2}\epsilon_0 V E^2 (\alpha_{\parallel} \sin^2 \theta + \alpha_{\perp} \cos^2 \theta) \cos^2 \varphi. \quad (22)$$

The necessary condition of extreme,

$$\frac{\partial U_e}{\partial \theta} = -\frac{1}{2}\epsilon_0 V E^2 (\alpha_{\parallel} - \alpha_{\perp}) \sin 2\theta \cos^2 \varphi = 0, \quad (23)$$

$$\frac{\partial U_e}{\partial \varphi} = \frac{1}{2}\epsilon_0 V E^2 (\alpha_{\parallel} \sin^2 \theta + \alpha_{\perp} \cos^2 \theta) \sin 2\varphi = 0$$

is satisfied if

$$\theta = 0 \text{ или } \pi/2, \text{ и } \varphi = 0 \text{ или } \pi/2.$$

The quadratic form

$$d^2U = \sum_{i=1}^2 \sum_{k=1}^2 \frac{\partial^2 U}{\partial x_i \partial x_k} \Delta x_i \Delta x_k,$$

where  $x_1 = \theta, x_2 = \varphi$ , is positively defined only at  $\theta = \pi/2$  and  $\varphi = 0$  for prolate ellipsoids of rotation, and only at  $\theta = 0$  and  $\varphi = 0$  for spheroids. These formulas correspond to the minimum of potential energy.

Right-hand sides in Eq. (23), taken with the opposite sign, represent the acting moments of forces. The directions of the moments are mutually orthogonal. The moment  $\partial U / \partial \varphi$  is directed along the  $z$  axis, i.e., vertically. It acts so that the rotations of the particles of some or another type will alined along the field direction. The moment  $\partial U / \partial \theta$  may have an arbitrary horizontal direction. Its action is analogous to the action of aerodynamic moment of forces, i.e., larger diameters tend to take the horizontal position. An example of joint action of electric and aerodynamic moments of forces on the oblate spheroids is shown in Fig. 4.

It is seen that, as the field intensity increases, the rotation angles are grouped closer around the vertical. In addition, the rotation axes of the prolate ellipsoids tend to orient along the direction of the field intensity vector. In Fig. 5 we can see how under the action of the field the uniform distribution over the azimuth angle is transformed to the concentration around the direction  $\varphi = 0$ .

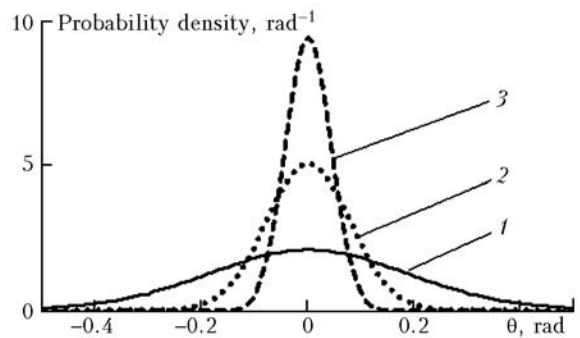


**Fig. 4.** Distribution over the angles of the polar orientation  $\theta$  of the axes of spheroids with sizes  $h = 50 \mu\text{m}$  and the ratio of semiaxes 2.5:1 for the horizontal gradient of electric field potential  $E = 0$  (curve 1),  $5 \cdot 10^3$  (curve 2); and  $10^4 \text{ V/m}$  (curve 3). The energy dissipation rate  $\epsilon = 5 \cdot 10^{-4}$ .

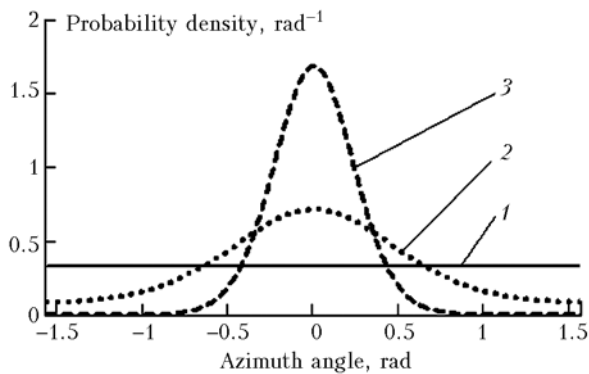


**Fig. 5.** Distribution of the azimuthal orientation of the rotation axes of the prolate ellipsoids in the presence of horizontal gradient of the potential of electric field  $E$  in the direction  $\varphi = 0$ :  $E = 0$  (curve 1),  $3 \cdot 10^2$  (curve 2), and  $10^3$  V/m (curve 3).

The turbulence is, as before, the main destructive factor, preventing strict orientation into the above-mentioned directions.

## Conclusion

We overviewed and concisely characterized the different physical factors influencing the ice cloud particle orientation. The estimates were made by the example of spheroidal and ellipsoidal particles, but it may be stated with confidence that they reflect the main regularities in behavior of plate and columnar particles. We studied in more detail the combined action of the aerodynamic moment of forces, arising during particle fall, and the moment of electrostatic potential in the atmosphere. It is shown that in the case of the vertical gradient of the potential of the order of  $10^3$  V/m or higher, there occurs separation by the distribution type in the polydispersion ensemble.

In the absence of the field, particles with large diameters oriented predominately in the horizontal direction, with increase of the field intensity, start to take the positions, when larger diameters become predominately vertical, first this takes place with small particles and then with bigger ones. The horizontal gradient of the potential increases the effect of the aerodynamic moment of forces, thereby favoring the establishment of more strict orientation by large diameters in the horizontal position. In addition, the horizontal gradient of the potential favors the azimuthal orientation of column-shaped particles, whose large diameters are oriented predominately in the direction of the electric field intensity vector.

## Acknowledgements

This work is supported by the Russian Foundation for Basic Research (Grants Nos. 07-05-00672, 06-05-89500 NNS, and 07-05-91102-AFGIR), as well as by Federal Agency for Science and Innovations (Governmental contract No. 02.518.11.7075).

## References

1. D.N. Romashov, *Atmos. Oceanic Opt.* **14**, No. 2, 102–110 (2001).
2. Y. Takano, K.N. Liou, and P. Minnis, *J. Atmos. Sci.* **49**, No. 7, 1487–1493 (1992).
3. K. Stephens, *J. Atmos. Sci.* **37**, No. 3, 435–446 (1980).
4. P. Yang and K.N. Liou, *J. Opt. Soc. Am. A* **12**, No. 1, 162–176 (1995).
5. V.V. Kuznetsov, N.K. Nikiforova, L.N. Pavlova, et al., *Trudy IEM*, Issue 7 (112), 101–106 (1983).
6. J. Zikmunda and G. Vali, *Observations of Fall Patterns for Natural Ice Crystals* (College of Engineering, Univ. Wyoming, Rep. N. AR103, 1972), 49 pp.
7. H.-R. Cho, J.V. Iribarne, and W.G. Richards, *J. Atmos. Sci.* **38**, No. 5, 1111–1114 (1981).
8. J.D. Klett, *J. Atmos. Sci.* **52**, No. 12, 2276–2285 (1995).
9. B.V. Kaul, S.N. Volkov, and I.V. Samokhvalov, *Atmos. Oceanic Opt.* **16**, No. 4, 325–332 (2003).
10. B.V. Kaul and I.V. Samokhvalov, *Atmos. Oceanic Opt.* **18**, No. 11, 866–870 (2005).
11. B.V. Kaul and I.V. Samokhvalov, *Atmos. Oceanic Opt.* **19**, No. 1, 38–42 (2006).
12. B.V. Kaul, *Atmos. Oceanic Opt.* **19**, No. 10, 751–755 (2006).
13. B.V. Kaul, *Izv. Vyssh. Uchebn. Zaved. SSSR. Ser. Fiz.*, No. 11, 17–21 (1983).
14. L.D. Landau and E.M. Livshits, *Theoretical Physics. Vol. VI. Hydrodynamics* (Fizmatlit, Moscow, 2001), 731 pp.
15. L.M. Miln-Tompson, *Theoretical Hydrodynamics* (Mir, Moscow, 1964), 497 pp.
16. P.K. Wang and Wusheing Ji, *J. Atmos. Sci.* **54**, No. 18, 2261–2274 (1997).
17. O.A. Volkovitskii, L.N. Pavlova, and A.G. Petrushin, *Optical Properties of Ice Clouds* (Gidrometeoizdat, Leningrad, 1984), 198 pp.
18. W.P. Arnott and J. Hallett, in: *Cirrus: OSA Technical Digest* (Washington DS, 1998), pp. 86–88.
19. A.J. Reynolds, *Turbulent Flows in Engineering Applications* [Russian translation] (Energiya, Moscow, 1979), 405 pp.
20. K. Langgenhager, *Zeitschrift für Meteorol.* Bd 27, H. 3, 179–183 (1977).
21. A.R. Hippel, *Dielectrics and Waves* [Russian translation] (Nauka, Moscow, 1960), 271 pp.
22. I.M. Imyanitov, E.V. Chubarina, and Ya.M. Shvarts, *Electricity of Clouds* (Gidrometeoizdat, Leningrad, 1970), 93 pp.